Bull. Chem. Soc. Ethiop. **2026**, 40(10), 2173-2183.
DOI: https://dx.doi.org/10.4314/bcse.v40i10.9

ISSN 1011-3924
Printed in Ethiopia
Online ISSN 1726-801X

α-AMINO NITRILE COMPLEXES of Cr, Co, Ni, AND Cu: SYNTHESIS, CHARACTERIZATION, AND BIOLOGICAL EVALUATION

Aseel H. Abad Al-Ameer

Department of Chemistry, College of Science, University of Baghdad, Baghdad 64021, Iraq

(Received May 7, 2026; Revised June 7, 2026; Accepted June 22, 2026)

ABSTRACT. Many studies have been conducted in the field of α-amino nitrile complexes. A new series of metal ion complexes for Cr(III), Co(II), Ni(II), and Cu(II) was derived from the α-aminonitrile 2-(2-hydroxyphenyl)-2-(o-tolylamino)acetonitrile ligand (HL). The complexes have been characterized using conventional techniques such as (FT-IR), (UV-VIS) spectroscopy, (C.H.N.M), metal chlorides, thermal analysis, ^{1}H-NMR, molar conductivity and magnetic moment. Octahedral geometries were suggested for the new complexes, while the Ni-complex was suggested as a pseudo-tetrahedral geometry, according to the magnetic moment value (3.11 B.M.) and the electronic spectrum; they were observed to be electrolytic. The coordination behavior of the ligand was bidentate, of the NO-type, through hydroxyl and amine groups. Antibacterial activity has been evaluated for the synthesized compounds against *Pseudomonas, Escherichia coli, Proteus, and Staphylococcus aureus*; the results were promising, considering the presence of a free nitrile moiety and metal ions, which influenced the structure-activity relationship. Antioxidant activity was observed using the DPPH assay, where the ligand and complexes exhibited radical scavenging activity IC_{50}% in the range of (0.012-0.005) compared to gallic acid. Anticancer activity studies revealed that the Cu(II) complex showed the highest cytotoxicity with the lowest IC_{50} value (224.67 µM), indicating enhanced activity upon complexation.

KEY WORDS: α-Aminonitrile, Bi-dentate ligand, Anti-bacterial activity, Electrolytic

INTRODUCTION

A one-pot multi-component condensation reaction is important because it can accomplish several bond-forming processes in a single vessel. The Strecker reaction, discovered in 1850 [1], was the first multi-component reaction. In the Strecker reaction, a carbonyl compound (an aldehyde), an amine, and hydrogen cyanide combine to form an α-aminonitrile with an intermediate that forms as a latent imine [2]. α-Aminonitriles serve as valuable intermediates in organic syntheses. They have been extensively used as precursors for amino acids and amide synthesis [3]. Furthermore, several studies have confirmed their application in the synthesis of a variety of nitrogen-containing heterocyclic compounds, including triazoles and tetrazoles [4]. Many research studies were carried out on their application in the formation of nitrogen heterocycles like triazoles, tetrazoles, and amidines [5]. Other researchers utilized Strecker-derived α-aminonitriles for forming different heterocycles like imidazole, 1,2-diamines, and thiadiazols [6, 7]. α-Aminonitriles are versatile intermediates in organic synthesis. They have been widely employed as precursors for the preparation of amino acids and amino amides [3]. In addition, several studies reported their use in the synthesis of nitrogen-containing heterocyclic compounds, including triazoles, tetrazoles, and amidines [5]. Other researchers demonstrated that Strecker-derived α-aminonitriles can be transformed into various heterocyclic systems such as imidazoles, 1,2-diamines, and thiadiazoles, expanding their utility in medicinal and synthetic chemistry [6, 7].

Medically, αaminonitriles are involved in synthesizing hepatitis C virus NS3 serine protease inhibitors via diastereoselective Strecker reactions [8], and in the creation of compounds such as (±) phthalascidin 622 (Saframycin A analog) [9] and novel boron-containing retinoids [10].

*Corresponding authors. E-mail: aseel.h@sc.uobaghdad.edu.iq

Typically, α-aminonitriles are synthesized by reacting an imine with a cyanide source, such as HCN, KCN, $(EtO)_2P(O)CN$ [20], Et_2AlCN [11], Bu_3SnCN, or Me_3SiCN [12]. The Strecker reaction has also seen some modifications with different catalysts from the literature, including inorganic and organic [13] ones. The reaction has also been modified for greener chemistry approaches using water and ionic liquids as solvents. After the initial synthesis of α-aminonitriles, a number of reports have explored the biological activity of this compound. The compound and its analogs are still under investigation because of their potential applications in cancer and tumor treatment, as the nitrile group is of crucial importance in such applications [14]. Transition-metal complexes derived from these compounds have also been studied for their industrial role. In this study, we designed an NO-type bidentate αaminonitrile ligand [15] and examined its interactions with various metal ions to identify the coordination sites and donor group behaviors. Continuing our research, we subjected a new series of metal ions to coordination with this ligand. Due to the limited research on α-aminonitrile ligation, we aim to contribute to this underexplored area and encourage further investigation by other researchers.

EXPERIMENTAL

Materials and methods

The chemicals were used as such without any purification. The melting points of the synthesized complexes were determined using the open capillary method, and the apparatus used was a Gallenkamp hot stage melting point apparatus. The micro elemental analysis was done using a EuroEA CHN instrument. The metal content in the complexes was estimated using an Agilent Varian AA 240 FS FAAS instrument, and nitrous oxide was used as the gas in the estimation of chromium. The magnetic susceptibility at room temperature was determined using a Johnson Matthey Catalytic Systems Division Magnetic Susceptibility Balance.

Synthesis of α-aminonitrile ligand (HL)

The 2-(2-hydroxyphenyl)-2-(o-tolylamino) acetonitrile ligand (HL) was synthesized according to the literature in previous work [16]. 0.01 mole of o-hydroxy benzaldehyde was dissolved in 20 mL of glacial acetic acid, followed by the addition of 0.02 mol of o-toluidine. The imine compound was prepared, and the pH value was adjusted to near 4 by the addition of conc. sulfuric acid drop by drop, the color changed to orange, and then 0.01 mol of potassium cyanide was added to the mixture, which was then refluxed and stirred overnight. HL was separated after neutralizing the medium with ammonia solution, then filtration. It is a brown solid of chemical formula $C_{15}H_{14}N_2O$. It possesses NO-type chelating property; it is considered a bidentate chelator ligand as shown in Scheme 1.

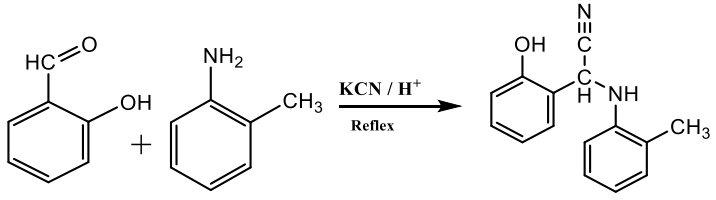

2-hydroxybenzaldehyde *o*-toluidine 2-(2-hydroxyphenyl)-2-(*o*-tolylamino)acetonitrile

Scheme 1. Synthesis of HL ligand.

Synthesis methods of C1-C4 complexes

One mmol of $CrCl_3.6H_2O$, $CoCl_2.6H_2O$, $NiCl_2.6H_2O$and $CuCl_2.4H_2O$ salts were dissolved in 10 mL of ethanol, then added drop by drop to 2 mmol of the ligand (HL), which was dissolved in 10 mL of absolute ethanol previously, as shown in Scheme 2. The resulting mixture was refluxed for 3 hours to synthesize C1-C4 complexes, respectively. The precipitates were collected by filtration, then dried and stored in a desiccator [17].

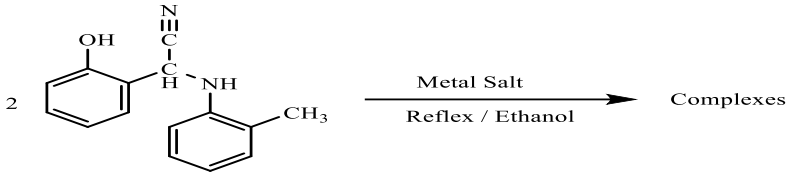

2-(2-hydroxyphenyl)-2-(*o*-tolylamino)acetonitrile (HL)

Metal Salt = Cr^{+3}, Co^{+2},Ni^{+2},Cu^{+2}

Scheme 2. Reaction of HL ligand with suggested metal salts.

RESULTS AND DISCUSSION

The significance of preparing α-aminonitrile compounds lies in their versatility as key precursors for synthesizing a wide range of compounds. The structures of the prepared complexes were characterized using FT-IR and UV-Visible spectroscopy, metal and elemental (C, H, N) analysis, molar conductivity, and thermal analysis. Symbol, formula, some physical properties, and yield percentage of the prepared complex compounds were listed in Table 1.

Table 1. Analytical and physical data of ligand (HL) and complexes (C1-C4).

Symbol	Chemical formula and molecular weight	Color	Melting point (ºC)	Yield%	C% calc. (found)	H% calc. (found)	N% calc. (found)	M% calc. (found)	Cl% calc. (found)
HL	$C_{15}H_{14}N_2O$ 238.3 g/mol	pale yellow	220-224	75.23	75.53 (74.55)	5.89 (4.98)	11. 74 (11.10)	6.73 (6.79)	-------
C1	$[Cr(HL)_2(H_2O)_2]Cl_3.4H2O$ 744.00 g/mol	Green	184-187	86.4	56.44 (56.41)	4.25 (4.22)	13.09 (11.29)	5.81 (5.28)	5.33 (6.11)
C2	$[Co(HL)_2Cl(H_2O)]Cl.H_2O$ 624.60 g/mol	Dark-green	190-194	77.12	52.23 (52.37)	4.70 (5.10)	12.18 (11.92)	5.65 (5.44)	5.29 (6.28)
C3	$[Ni(HL)_2(H_2O)_2]Cl_2.2H_2O$ 678.20 g/mol	Brown -green	200-205	79.34	58.60 (57.53)	4.44 (5.10)	12.67 (11.81)	6.87 (6.30)	4.17 (5.83)
C4	$[Cu(HL)_2(H_2O)_2]Cl_2.5H2O$ 737.10 g/mol	Brown	246-250	83.00	59.03 (60.00)	4.35 (5.10)	13.76 (12.76)	6.80 (6.62)	4.84 (4.71)

Infrared spectral studies

A comparative study was conducted for the FT-IR spectra of the synthesized complexes, as well as the free ligand (HL), using a Shimadzu 8300 FT-IR spectrophotometer. Table 2 presents the FT-IR bands for all the synthesized compounds, emphasizing the major bands. The possible sites for coordination were the secondary amine, phenolic hydroxyl, and nitrile groups. However, the shifts observed for the bands of the complexes, relative to the free ligand, indicated bidentate chelating modes, as indicated by the NO-type of coordination. Evidence for the coordination of the hydroxyl and amine groups is indicated by the shift of the bands [41]. However, non-neutral complexes usually include lattice water, which is indicated by a broad band at 3430-3400 cm^{-1}, thereby overlapping with the bands for υ(O-H) and υ(N-H), which may be difficult to identify. However, the bending modes for the amino groups, indicated by δ(N-H), shifted to lower and upper wavenumbers by approximately 28-7 cm^{-1}. On the other hand, the nitrile groups, indicated by -C≡N, shifted to lower wavenumbers by approximately 99-145 $cm^{-1,}$ attributed to the disruption of the intramolecular hydrogen bonds involving the hydroxyl groups upon coordination [18-20].

Table 2. Characteristic infrared absorption bands of the ligand (HL) and complexes (C1-C4).

	Compound	*υ*(OH)	*υ*(NH) amine	*υ*(C≡N) nitrile	δ(NH)	*υ*(C=C) aromatic	Out of plain deformation		
							mono sub.	ortho sub.	Para sub.
HL	HL	3427	3390	2210	1512	1604	624	754	860
C1	$[Cr(HL)_2(H_2O)_2]Cl_3.4H_2O$	3400 broads	Masked	2217	1533	1601	650 720	712	855
C2	$[Co(HL)_2Cl(H_2O)]Cl.H_2O$	3396 broad	3371	2241	1541	1599	642 714	756	802
C3	$[Ni(HL)_2(H_2O)_2]Cl_2.2H_2O$	3400-broad	3289	2240	1504	1601	685 715	736	846
C4	$[Cu(HL)_2(H_2O)_2]Cl_2.5H2O$	3342 broad	3232	2231	1528	1591	689, 707	757	842

Electronic spectra, magnetic moment, and molar conductivity of C1–C4 complexes

All of the complexes (C1-C4) have bands in the UV-Vis region. Electronic spectra of all complexes were recorded in DMSO using a Shimadzu UV-Vis 160A spectrophotometer with wavelengths ranging from 200-1100 nm. Two bands for HL appear at 325 nm and 297 nm due to n → π* transitions of non-bonding electrons and π → π* transitions of aromatic groups, respectively. For the ligand-to-metal charge transfer band at 357 nm. For the Cr(III) complex (C1), two bands in DMSO appear at 696 nm and 423 nm corresponding to $^4A_2g(F) \rightarrow {}^4T_2g(F)$ (ν1) and $^4A_2g(F) \rightarrow {}^4T_1g(F)$ (ν2) transitions, indicating octahedral geometry. Two bands for HL appear at 294 nm and 277 nm due to n → π* and π → π* transitions, respectively. For the Cr(III) complex, the magnetic moment is 3.80 B.M., indicating three unpaired electrons in the metal center. The dark green color of the complex is in accordance with its structure. For the Co(II) complex (C2), two bands in DMSO appear at 696 nm corresponding to $^4T_{1g} \rightarrow {}^4T_2g$, (ν1) and 422 nm $^1A_1g \rightarrow {}^1T_2g$ (ν2) transitions. Two bands for HL appear at 251 nm and 335 nm due to π → π* transitions of non-bonding electrons and n → π* transitions, respectively. For the Ni(II) complex, the magnetic moment value (3.11 B.M.), in addition to the electronic spectrum, shows a broad band at 696 nm, assignable to the $^3T_1(F) \rightarrow {}^3T_1(P)$ transition. The absence of well-resolved multiple bands may be attributed to band overlapping and solvent effects in DMSO. Therefore,

the geometry around the Ni(II) center may be described as a slightly pseudo-tetrahedral geometry [21]. The Cu(II) complex C4 has an absorption band at 822 nm, corresponding to the ^2T_2g to ^2Eg transition. It indicates an octahedral geometry. For ligand HL, there is an absorption band at 336 nm, 245nm corresponding to the (n to π *) and (π to π *) transition [22]. Table 3 and Figures (1 - 4) summarize all the results from the complexes.

Table 3. Electronic transitions, molar conductance, and suggested structure of C1-C4 complexes.

	Compound formula and symbol	λ (nm)	ύ (cm^{-1})	Assignments	Conductivity in DMSO	Mef (BM)	Suggested structure
	HL	325 297 357	30769 33670 28011	n → π * π → π * L→ M (CT)			
C1	$[Cr(HL)_2(H_2O)_2]$ $Cl_3.4H_2O$	696 423 294 277	14367 23640 24013 36101	$^4A_2g(F) \rightarrow ^4T_2g(F)$ $^4A_2g(F) \rightarrow ^4T_1g(F)$ n → π * π → π *	92	3.80	Octahedral
C2	$[Co(HL)_2Cl(H_2O)]$ $Cl.H_2O$	699 422 335 251	14306 23696 29850 39840	$^4T_{1g} \rightarrow ^4T_2g$, $^4T_{1g} \rightarrow ^4T_1g(p)$, n → π * π → π *	61	4.56	Octahedral
C3	$[Ni(HL)_2]$ $Cl_2.2H_2O$	696 353 293	14367 28326 34129	$^3T_1 \rightarrow ^3T_1(p)$ n → π * π → π *	37	3.11	pseudo-tetrahedral geometry,
C4	$[Cu(HL)_2(H_2O)_2]$ $Cl_2.5H2O$	822 336 245	121654 29761 40816	$^2T_2g \rightarrow ^2Eg$ n → π * π → π *	83	3.76	Octahedral

Thermal analysis

The thermal study of cobalt complex $[Co(HL)_2Cl(H_2O)]Cl{\cdot}H_2O$ was carried out using thermogravimetric analysis (TGA), as presented in Figure 1. The decomposition of this complex takes place in two steps when exposed to air. The complex loses weight over time and temperature (0-290 °C), where gases are released through dehydration, loss of lattice and coordinated water molecules, and chloride ions. In the second step, when the temperature is increased, a major loss of weight is observed, where the ligand part of the complex is lost, present at both ends of two ligands. The residue is cobalt oxide, showing good coordination between ligands and metals, indicating good stability of the complex. Table 4 and Figure 5 present temperature ranges, weight loss, and fragments lost during decomposition [23].

Table 4. Thermal decomposition data of cobalt complex (C2).

Complex	Temp. range, °C	Weight lost %		Remaining part	Liberated part
		Found	Calc.		
C2 $[Co(HL)_2Cl(H_2O)]$ $Cl.H_2O$	0-140	8.10	8.56	$[Co(HL)_2Cl(H_2O)]$	$[H_2O]$ Lattice water + Cl
	140-290	14.73	13.96	$[Co(HL)_2]$	$[H_2O, Cl_2]$ gases
	290-780	76.20	76.25	CoO	2HL

^{1}H-NMR HL ligand

The ligand 2-(2-hydroxyphenyl)-2-(o-tolylamino) acetonitrile ligand (HL). was analyzed by ^{1}H and ^{13}C-NMR spectroscopy, with DMSO-d_6 as the solvent. The ^{1}H-NMR spectrum showed the presence of four sets of peaks. The CH_3 protons were seen as a doublet at 1.0 ppm (2H). The aromatic protons were seen as a series of peaks within the range of 7.2 -8.5 ppm. The N–H peak was seen as a singlet at 9.0- 10.3 ppm (1H). The O–H peak was seen as a singlet at 11.12 ppm (1H). The solvent peaks were seen as a singlet at 2.5ppm (1H, water) and as a singlet at 3.3 ppm (1H, non-deuterated DMSO)[24].

Table 5. ^{1}H-NMR chemical shifts, multiplicity, and assignments of HL.

HL	δ (ppm)	Multiplicity	Integration	Assignment
^{1}H-NMR	1.0	doublet	2H	CH_3
	7.2 -8.5	Mutiplet	5H	Ar-H
	11.12	Singlet	1H	HO-Ph
	9.0- 10.3	Singlet	1H	NH-Ph
	2.5-3.3	Singlet	1H	DMSO+H_2O

4- *In vitro antibacterial activity*

The study aimed at determining the antibacterial potential of the α-aminonitrile ligand HL and its complexes against four microbial species: Gram-negative *Pseudomonas spp*., *Escherichia coli*, *Proteus spp*., and Gram-positive *Staphylococcus aureus*. The antibacterial screening was carried out using the well diffusion method. The results were obtained in millimeters. The cultures were incubated at 37°C for 18 hours. The ligands were dissolved in DMSO at a concentration of 10^{-3}M. Tetracycline was used as the Gram-negative and Gram-positive control. The inhibition zone refers to the clear region surrounding the disc where no microbial growth is observed. Table 6 presents the antibacterial screening results for the ligand and its complexes against the four microorganisms. The results show that metal complexes have greater antibacterial potential than the free ligand against Gram-negative *Pseudomonas spp.* and *Proteus spp.* The increased potential can be explained by the effective coordination of the metal ions and the appropriate alignment with the ligand's orbitals to minimize polarity and increase electron delocalization in the chelate ring. The increased potential allows for the penetration of the lipid layer and protection of the metal-binding sites in the microbial enzymes. The ligand's structure also plays a role in the increased potential since it is known for its antibacterial and antifungal activities. The activities include those associated with the nitrile group [25-28].

Table 6. Antibacterial activity of HL ligand and its complexes against tested microorganisms at a concentration of 10^{-3} M.

Compound	*Pseudomonas spp.* G^-		*Escherichia coli* G^-		*Proteus spp* G^-		*Staphylococcus aureus* G^+	
	activity	zone (mm)	activity	zone (mm)	activity	zone (mm)	activity	zone (mm)
C1	++	14	++	16	++	14	++	13
C2	++	12	++	15	++	13	++	16
C3	++	16	---	---	++	14	++	19
C4	++	14	++	11	++	11	++	14
HL	---	---	++	18	---	---	+++	22
DMSO (Control)	++	11	---	---	++	11	---	---

Tetracycline	---	---	+++	26	---	---	---	---

Antioxidant activity

The purpose of this assessment was to evaluate the efficacy of antioxidants in scavenging DPPH free radicals. The antioxidants donate hydrazine or hydrogen, which reacts with the singly occupied nitrogen in the DPPH free radicals. Gallic acid was used as a sample compound to evaluate the antioxidant potential of the complexes. The antioxidant activity was carried out using the DPPH assay. An equal volume of concentrated DPPH solution containing 0.135 mM was added to each of the diluted antioxidants. The hydrazine-associated color changed to yellow as a result of the reaction with the antioxidants. The reaction mixtures were then left at room temperature in the dark for 30 minutes after adding the DPPH solution. The absorbance was then measured at 517 nm for each of the reaction mixtures. The complexes showed significant free radical scavenging activity relative to the standard compound, as demonstrated by low IC_{50} values. The free radical scavenging activity is as follows: Gallic acid > Cu-complex > Cr-complex > Ni-complex > Ligand > Co-complex. All complexes and ligands showed low IC_{50} values, but the standard compound, Gallic acid, was the best one according to the (low IC_{50} 0.004 and high PI% 68.16). The interaction of complexes with DPPH radicals is shown in Table 7. The complexes donate hydrazine or hydrogen, which reacts with DPPH free radicals that are then scavenged. [29-32].

Table 7. The antioxidant results PI% (Percentage of Inhibition) and IC_{50} of the ligand and its metal complexes.

IC_{50} µg/mL	PI%	Concentration µg/mL	
0.004	18.73	0.008	Gallic acid
	45.69	0.004	
	60.35	0.002	
	68.16	0.001	
0.012	11.63	0.008	Ligand
	30.34	0.004	
	39.42	0.002	
	45.06	0.001	
0.009	30.43	0.008	C1
	41.43	0.004	
	47.33	0.002	
	50.19	0.001	
0.015	24.09	0.008	C2
	35.75	0.004	
	44.16	0.002	
	47.62	0.001	
0.011	24.09	0.008	C3
	35.75	0.004	
	44.16	0.002	
	47.62	0.001	
0.005	24.43	0.008	C4
	36.82	0.004	
	44.96	0.002	
	47.62	0.001	

Anti-cancer study of the cytotoxicity of complexes

Cytotoxicity of the ligand and its complexes was carried out by the standard MTT assay, and the experiment was done at four different concentrations: 22.22, 66.66, 200, and 600 µg/mL, on the

MCF-7 breast cancer cell line. Absorbance was recorded at 570 nm, and two readings were taken for each concentration, followed by the calculation of the mean after 24 hours. Different IC_{50} values were obtained, as depicted in Table 8. Among the complexes, the copper complex had the lowest IC_{50}, indicating that it was the most effective in killing the cancer cells [33-36].

Table 8. Cytotoxicity of ligand and complexes towards MCF-7.

Sample ID	Concentration (µg/mL)	Absorption at 570 nm	IC_{50}
HL	22.22	0.335	242.90 µg/mL
	66.66	0.332	
	200	0.307	
	600	0.171	
C1	22.22	0.352	254.60 µg/mL
	66.66	0.361	
	200	0.308	
	600	0.270	
C2	22.22	0.335	244.91 µg/mL
	66.66	0.322	
	200	0.301	
	600	0.179	
C3	22.22	0.352	234.66 µg/mL
	66.66	0.361	
	200	0.308	
	600	0.270	
C4	22.22	0.357	224.67 µg/mL
	66.66	0.363	
	200	0.347	
	600	0.265	

CONCLUSIONS

The Integrated α-aminonitrile ligand (HL) involves multiple potential donor sites; however, it coordinates in a bidentate manner through the nitrogen and oxygen atoms, making stable six-membered chelate rings with the metal ions in a 1:2 (M: L) ratio. The residual coordination sites are occupied by water molecules and/or chloride ions, completing the coordination sphere. Based on the spectral, analytical, and magnetic data, the Cr(III), Co(II), and Cu(II) complexes are proposed to adopt octahedral geometries, while the Ni(II) complex is best designated as having a pseudo-tetrahedral environment. The recommended chemical formulas are $[Cr(HL)_2(H_2O)_2]Cl_3\cdot 4H_2O$, $[Co(HL)_2Cl(H_2O)]Cl\cdot H_2O$, $[Ni(HL)_2]Cl_2\cdot 2H_2O$, and $[Cu(HL)_2(H_2O)_2]Cl_2\cdot 5H_2O$. Coordinated and lattice water molecules exist in some complexes, as supported by thermal analysis. The denoted structures are explained in Figure 10. The antibacterial activity of the ligand and its complexes was evaluated against *Escherichia coli*, *Staphylococcus aureus*, *Pseudomonas aeruginosa*, and *Proteus spp*. The ligand exhibited strong inhibition against *E. coli* and *S. aureus*, while the metal complexes generally developed activity against most tested strains. On the other hand, the Ni(II) complex (C3) showed relatively lower activity against *E. coli*. The enhanced activity of the complexes compared to the free ligand may be attributed to chelation, which increases lipophilicity and facilitates penetration through microbial cell membranes. Antioxidant activity was assessed using the DPPH radical scavenging method, with gallic acid as a reference standard. The IC_{50} values indicate that gallic acid exhibits the highest antioxidant activity, followed by the Cu(II) complex, Cr(III) complex, Ni(II) complex,

ligand, and Co(II) complex. This reflects the influence of metal coordination on radical scavenging efficiency. Cytotoxicity studies revealed that the Cu(II) and Ni(II) complexes exhibit the most significant anticancer activity, as indicated by their lower IC_{50} values compared to the ligand and other complexes. This suggests that complexation enhances the biological activity, likely due to improved cellular uptake and interaction with biomolecular targets.

ACKNOWLEDGMENT

Thanks to the Department of Chemistry, College of Science, University of Baghdad, Iraq for offering many books and research equipment.

REFERENCES

1. Abtew, E.; Domb, A.J. Synthesis of polypeptides and poly (α-hydroxy esters) from aldehydes using Strecker synthesis. *ACS Omega* **2023**, 18, 40407-40416.
2. Misganaw, K.; Thillairasu, P.; Shumi, G.; Debebe, H.; Berhanu, S. Vanillin and 4-nitroanilline derived schiff-base and its nickel(II) complex: Spectral analysis and antibacterial investigation. *Bull. Chem. Soc. Ethiop.* **2024**, 38, 1275-1289.
3. Cheewawisuttichai, T.; Hurst, R.D.; Brichacek, M. Transformation of aldehydes into nitriles in an aqueous medium using O-phenylhydroxylamine as the nitrogen source. *Carbohydr. Res*. **2021**, 502, 108282.
4. Ganesan, M.; Nagaraaj, P. Recent developments in dehydration of primary amides to nitriles. *Org. Chem. Front*. **2020**, 7, 3792-3814.
5. Alfano, A.I.; Sorato, A.; Ciogli, A.; Lange, H.; Brindisi, M. Enantioselective catalytic Strecker reaction on cyclic (Z)-aldimines in flow: Reaction optimization and sustainability aspects. *J. Flow Chem*. **2024**, 14, 197-210.
6. Ali, D.N.; Khaleel, A.M. Synthesis of new Schiff base of ciprofloxacin derivative with its Cu(II), Ag(I) and Pt(IV) complexes and evaluation of antibacterial activity. *Biochem. Cell. Arch*. **2020**, 20, 2441-2448.
7. Abd Al-Ameer, A.H. Metal complexes of mixed ligands (quinolone antibiotics and α-aminonitrile derivatives) their applications: An update with Fe(III), Co(II) and Ni(II) ions and study the biological activity. *JGPT* **2019**, 11, 515-524.
8. Ghorbanpour, M.; Soltani, B. An updated overview on nitrogen-rich azole-based gold coordination complexes as potent anticancer agents. *Coord. Chem. Revi*. **2025**, 523, 216233.
9. Huang, J.; Huang, J.; Wang, N.; Wang, L.; Li, L.; Wang, C.; Sun, X.; Li, Y.; Huang, G.; Ma, X. Identification of 2 (1H)-pyrimidinones as potential EGFR T790M inhibitors for the treatment of gefitinib-resistant non-small cell lung cancer. *Bioorg. Chem.* **2019**, 89, p.102994.
10. Ghani, A.H.; Alabdali, A.J. Synthesis, characterization and anti-cancer activity of gold(III) and nickel(II) metal ion complexes derived from tetrazole-triazole compound. *Al-Nahrain J. Sci*. **2022**, 25, 8-13.
11. Al-Ameer, A.H.A. Synthesis and characterization of new complexes of 2- (benzo[d]thiazol-2- ylamino)-2-(5-chloro-2-hydroxy phenyl) acetonitrile ligand with some divalent transition metal ions. *Res. J. Chem. Environ.* **2019**, 23, 170-175.
12. Ajibulu, K.E.; Okoronkwo, A.E.; Owolabi, J.B.; Oyetayo, V.O. Synthesis, characterization, antimicrobial and toxicological study of Mn(II), Ni(II) complexes of tridentate ligand derived from ethylenediamine, chlorobenzalde-hyde and aminobenzophenone. *IJESIR* **2023**, 4, 01000148.
13. Alabdali, A.J; Al-Amery, M.H.A. Synthesis, thermal study and biological activity of cobalt (II) and copper(II) mixed ligand complexes using (n-4-methoxy phenyl) amino phenyl acetonitrile and histidine ligands. *J. Pharm. Sci. Res*. **2019**, 11, 155-158,

14. Masamba, W.; Petasis, vs. Strecker amino acid synthesis: Convergence, divergence and opportunities in organic synthesis. *Molecules* **2021**, 26, 1707.
15. Al-Ameer, A.H. Preparation, characterization and antibacterial studies of Schiff base derivatives with 4-bromo-2.6-dimethylaniline and study their complexes with some transition metal ions. *Int. J. Drug Deliv. Technol*. **2021**, 11, 190-194.
16. Obaid, S.M.H.; Abd-Almonuim, A.E.; Al-Naymi, H.A.S.; Jarad, A.J.; Saleh, M.M. Synthesis and characterization of some metal ions complexes with mixed ligand of azo dye and metformin and evaluation of its effectiveness on the growth of some pathogenic bacteria clinically isolated and study of its toxicity on normal and cancerous hepatocytes. *Heliyon* **2024**, 10, e37849.
17. Ghogare, R.S. Succinic acid: a novel and efficient organo-catalyst for synthesis of α- amino nitriles under solvent free condition. *Org. Commun*. **2020**, 13,103-113.
18. Mashhadi, M.; Shiri, S.A. Natural halloysite nanotubes as an efficient catalyst in strecker reaction: the synthesis of α-amino nitriles under solvent-free conditions. *Mol. Divers*. **2023**, 27, 919-929.
19. Manhee, T.Q.; Alabdali, A. J. Synthesis, characterization and anticancer activity of Ni(II), Cu(II), Pd(II) and Au(III) complexes derived from novel Mannich base. *Vietnam J. Chem.* **2024**, 62, 201-210.
20. Fadhel, A.M.; Al Hamdani, A.A.S.; Mohamed, S.G. Synthesis, characterization and antioxidant study of some metal ion complexes with azo 1-(2,4,6-trihydroxy-3-((3-hydroxyphenyl) diazenyl) phenyl) ethan-1-one, *Baghdad Sci. J.* **2024**, 21, 3642-3660.
21. Frampton, A. K.; Gartland, K.; Piro, N. A.; Kassel, W. S.; and Dougherty, W. G. Structural characterization and electrochemical properties of nickel (II) complexes bearing sterically bulky hydrotris (3-phenyl)-and hydrotris (3-tert-butylpyrazol-1-yl) borato ligands. *Polyhedron* **2016**, 114, 172-178.
22. Mohamed, E.A.; Negm, N.A.; Youssef, A.O.; Sayed, G.H. Preparation, characterization, and spectroscopic properties of a novel iron(III), copper(II), and nickel(II) complexes with Schiff base ligand derived from salicylaldehyde and *p*– phenylene diamine on polyvinyl chloride photodegradation. *Egypt. J. Chem.* **2024**, 67, 225-238.
23. Zhang, Q.; Liu, J. L.; Feng, X. X.; Liu, J. C. Nitrile-containing copper(II) porphyrin coordination complexes for efficient anticancer activity and mechanism research. *New J. Chem.* **2021**, 45, 5221-5227.
24. Hassan, S.S.; Hassan, N.M.; Baqer, S.R.; Saleh, A.M. Biological evaluation and theoretical study of bi-dentate ligand for amoxicillin derivative with some metal ions. *Baghdad Sci. J.* **2021**, 18, 1269-1278.
25. Alabdali, A.J.; Al-Ameer, A.H.A. New complexes of α-amino nitrile with VO(II), Cr(III), Fe(II), Fe(III), and Cd(II) metal ions: Synthesis, characterization and anti-bacterial activity. *Bull. Chem. Soc. Ethiop*. **2026**, 40, 443-453.
26. Al-Ameer, A.H.A. Synthesis, characterization and antibacterial studies of mixed ligand complexes of 2-phenyl-2-(O-tolylamino) acetonitrile and quinolone antibiotics with Ni(II), Cu(II), Zn(II) divalent metal ion complexes. *AIP Conf. Proc*. **2023**, 2414, 050001.
27. Al-Ameer, A.H.A.; Shaalan, N. Synthesis, spectroscopic, thermal, biological activities studies for Ni(II), Cu(II) and Zn(II) complexes with phthalohydrazide derived ligand and evaluation as antioxidants. *Bull. Chem. Soc. Ethiop*. **2025**, 39, 1109-1118.
28. Sharma, P.; Gogoi, A.; Verma, A.K.; Frontera, A.; Bhattacharyya, M.K. Charge-assisted hydrogen bond and nitrile⋯ nitrile interaction directed supramolecular associations in Cu(II) and Mn(II) coordination complexes: Anticancer, hematotoxicity and theoretical studies. *New J. Chem.* **2020**, 44, 5473-5488.
29. Gouda, M.A.; Attia, E.; Helal, M.H.; Salem, M.A. Recent progress on nicotinonitrile scaffold-based anticancer, antitumor, and antimicrobial agents: A literature review. *J. Heterocycl. Chem.* **2018**, 55, 2224-2250.

30. Oyamada, Y.; Fujii, M.; Takehara, T.; Suzuki, T.; Nakamura, S. Catalytic enantioselective construction of an α-thio-substituted α-aminonitriles-bearing tetrasubstituted carbon center. *ACS Catal.* **2024**, 14, 3411-3419.
31. Zhang, J.; Guo, M..; Chen, Y.; Zhang, S.; Wang, X.N.; Chang, J. Synthesis of amino-substituted α-and δ-carbolines via metal-free [2+ 2+ 2] cycloaddition of functionalized alkyne-nitriles with ynamides. *Org. Lett.* **2019**, 21, 1331-1336.
32. Al-Amery, M.H.; Rasheed, A.S.; Najeeb, D.A. Synthesis, spectral and antimicrobial investigation of 2-(naphthalenel-ylamino)-2-phenylacetonitrile and 1, 10-phenanthroline with five divalent transition metal ions. *Int. J. Pharm. Qual. Assur*. **2019**, 10, 40-46.
33. Nauth, A.M.; Konrad, T.; Papadopulu, Z.; Vierengel, N.; Lipp, B.; Opatz, T. Synthesis of α-aminonitriles using aliphatic nitriles, α-amino acids, and hexacyanoferrate as universally applicable non-toxic cyanide sources. *Green Chem*. **2018**, 20, 4217-4223.
34. Cai, S.; Ye, H.; Yang, X.; Ma, P.; Xu, S.; Zhang, Y. Aqueous phase synthesis of complex thiazole-containing peptides by condensation of N-acyl-α-aminonitriles and cysteine derivatives. *Org. Lett.* **2025**, 27, 12379-12384.
35. Sruthi, P.R.; Anas, S. An overview of synthetic modification of nitrile group in polymers and applications. *J. Polym. Sci.* **2020**, 58, 1039-1061.
36. Wright, T.B.; Turnbull, B.W.; Evans, P.A. Enantioselective rhodium-catalyzed allylic alkylation of β, γ-unsaturated α-amino nitriles: Synthetic homoenolate equivalents. *Angew. Chem.* **2019**, 131, 9991-9995.